Field-dressed orbitals in strong-field molecular ionization

Robert Siemering,[1] Oumarou Njoya,[2] Thomas Weinacht,[2] and Regina de Vivie-Riedle[1]
[1]*Department Chemie, Ludwig-Maximilians-Universität München, Butenandt Strasse 11, 81377 München, Germany*
[2]*Department of Physics and Astronomy, Stony Brook University, 100 Nicolls Road, Stony Brook, New York 11794-3800, USA*
(Received 20 April 2015; published 30 October 2015)

We demonstrate the importance of considering the shape of field-dressed molecular orbitals in interpreting angle-dependent measures of strong-field ionization from excited states. Our calculations of angle-dependent ionization for three homologous polyatomic molecules with very similar valence orbitals show that one has to take into account the shape of the field-dressed orbitals rather than the field-free orbitals in order to rationalize the experimental measurements.

DOI: 10.1103/PhysRevA.92.042515 PACS number(s): 31.15.ae, 33.80.Wz

Strong-field molecular ionization is at the forefront of current research on molecular structure and dynamics, particularly on attosecond time scales [1,2]. It is the first step in high-harmonic generation, which is used to generate attosecond light pulses, and it can be used to probe excited-state molecular dynamics as there are no dark states and one is not sensitive to the exact photon energy [3–8]. Furthermore, angle-resolved measurements of strong-field ionization have been shown to be sensitive to molecular structure and to reveal information about molecular orbitals from which electrons are removed during the ionization process [9–13].

Earlier work on small molecules demonstrated that angle-resolved strong-field ionization experiments showed angle-dependent yields that followed the calculated shapes of the highest occupied molecular orbital (HOMO) [14–17]. Other examples demonstrated the contributions from a superposition of the HOMO and the lowest unoccupied molecular orbital (LUMO) [18–20]. Molecular Ammosov-Delone-Krainov calculations of the angle-dependent ionization based on the calculated molecular or Dyson orbitals gave good agreement with the measured yields [21]. However, comparisons between calculation and experiment for larger systems have not been as favorable [22]. Furthermore, recent measurements on a series of molecules with similar molecular orbitals yielded different angle-dependent yields [23]. A recently developed method to calculate angular-dependent ionization probabilities based on electronic structure theory [20] seems flexible enough for larger systems.

In this work we demonstrate that it is the field-dressed molecular orbitals that provide insight into the angle dependence of the ionization yield. If the oscillations of the laser field are slow enough that the electrons in the molecule rearrange themselves as the field increases and decreases each half cycle, then the removal of an electron takes place from a Stark-shifted molecular orbital [24] and the shape of this orbital determines the angle dependence of the ionization yield.

We perform detailed calculations of the angle-dependent yield for three molecules from a homologous family: α-terpinene (AT), α-phellandrene (AP), and cyclohexadiene (CHD), which have calculated (measured) ionization potentials of 7.7 (7.6) eV, 8.0 eV, and 8.1 (8.2) eV, respectively. The calculations are for the molecules excited to their first bright neutral excited state, since this provides a natural method for aligning the molecules in experiment. In addition, the signal directly records the ionization probability of the molecule without a mapping step to the generated fragments as is often necessary in strong-field few-cycle experiments [25]. The calculations are compared with the measured yields and show remarkable agreement given the fact that the experiments have significant multiphoton character whereas the calculations are for pure tunnel ionization.

Measurements are performed using an amplified ultrafast titanium sapphire laser system in conjunction with an effusive molecular beam and time-of-flight mass spectrometer. The laser system produces 30-fs pulses with an energy of 1 mJ at a repetition rate of 1 kHz. Pump pulses at a central wavelength of 262 nm and a duration of 50 fs are generated via third-harmonic generation and focused in the molecular beam (to an intensity of about 0.3 TW/cm^2) to promote a fraction of the molecules to their first bright excited state. The molecules are probed with a more intense pulse at a central wavelength of 780 nm, focused to intensities between 5 and 10 TW/cm^2. The polarization of the pump pulses is varied with respect to the probe pulses by using a half wave plate, allowing us to vary the direction of the field of the ionization pulse relative to the transition dipole moment of the molecules. Molecular fragment ions are collected in a time-of-flight mass spectrometer. We measure the parent ion yield as a function of pump probe delay and polarization.

We calculated the angle-dependent ionization rates for the first optically excited states of CHD, AT, and AP. We performed quantum chemical calculations for the ground and the first three excited states with the MOLPRO program package [26] at the complete active space self-consistent field (CASSCF) (4,4) level of theory using the 6-31++G** basis set. The calculations were carried out with and without an external dipole field, which was added to the one-electron Hamiltonian to simulate the interaction with the strong-ionization field. The orientation of the molecules relative to the pump and probe polarization axes was included in the simulations.

The first angle φ is the rotation around the molecular transition dipole moment (TDM) axis and the second angle θ is the rotation around an axis perpendicular to the TDM axis, e.g., perpendicular to or in the molecular plane. These two angles are sufficient to describe all possible orientations between the molecule and the polarization vector of the incoming light fields. Both angles were varied in 10° steps.

The ionization probability of a molecule in a laser field can be modeled in terms of the induced electron flux through the barrier of the combined molecular and external electric field [27] (atomic units $m = \hbar = e = 1$ are used throughout

 ©2015 American Physical Society

the paper). This can be expressed as

$$W(t) = \int_S j(r,t)dS,$$
$$j(r,t) = -\frac{i}{2}[\psi(r,t)\nabla\psi(r,t)^* - \psi(r,t)^*\nabla\psi(r,t)]. \quad (1)$$

Here $j(r,t)$ is the electron flux density and $\psi(r,t)$ the electronic wave function in the presence of the electric field inducing the electron flux $W(t)$. For the surface S it is convenient to choose a plane perpendicular to the direction of the electric field. In our case S is located at the outer turning points of the electronic wave function. Here the wave function enters the classical forbidden region where tunneling occurs. The electronic wave functions, evaluated by a quantum chemical program package, are typically real and their flux density [Eq. (1)] is zero.

In Refs. [18,20] we showed that this problem can be overcome by evaluating the electron flux for the electron density $\rho(r,t)$ with the help of the divergence theorem and the continuity equation as proposed by [28]. We can then rewrite Eq. (1) as

$$W(t) = -\int_{V'} \nabla j(r,t)dV' = \frac{d}{dt}\int_{V'} \rho(r,t)dV', \quad (2)$$

with V' being the part of the total volume V in which the electronic wave function $\psi(r)$ is defined and which is spanned by the surface S and a vector perpendicular to S pointing away from the nuclei. In order to calculate the tunneling probability $T(S)$, we need the electron density with (at final time t_f) and without the external field (at initial time t_i). Therefore, we integrate Eq. (2) over time and obtain

$$T(t;S) = \int_{V'} \rho(r,t_f)dV' - \int_{V'} \rho(r,t_i)dV'. \quad (3)$$

In the present case, the tunneling probability $T(t;S)$ for the first optically excited state is sought. For CHD, low-lying Rydberg states in the Franck-Condon (FC) region have already been discussed in the literature [29,30]. We found low-lying Rydberg states in the FC region for the substituted CHD derivatives as well. In all three molecules the first excited state has Rydberg character and corresponds to an excitation from the HOMO to the LUMO (Rydberg). The optically active state is the second excited state, a $\pi\pi^*$ excitation (from the HOMO to the LUMO+1). Tunneling occurs mostly from the frontier orbitals and for our analysis we take into account the LUMO and the LUMO+1 orbitals from the state-averaged CASSCF calculation. Contributions from the HOMO are negligible.

To treat ionization from more than one orbital we solve the working equations derived above for a linear combination of the selected molecular orbitals. This implies a basis transformation rewriting the two orbitals (e.g., LUMO and LUMO+1) in the Slater determinant into the orbitals LUMO+LUMO+1 and LUMO–LUMO+1, allowing for coherent ionization of the electron from both orbitals [18,20].

This method is further extended to calculate tunnel ionization from excited states. Assuming the molecules are randomly oriented before the arrival of the pump pulse, the pump pulse introduces a $\cos^2$ distribution for the excited molecules with respect to the angle θ. Thus the molecules with a TDM along the laser polarization axis are excited preferentially. In addition, the rotation around φ has to be taken into account ranging from 0° to 360°, uniformly.

The pump and probe pulse are related by the polarization angle α. For a given delay time this angle is scanned between 0° and 180°. The probe pulse is responsible for the observed ionization. For a given α, the tunnel ionization probability $\tilde{T}(\alpha)$ is calculated as

$$\tilde{T}(\alpha) = \sum_{\varphi,\theta} \frac{1}{N}\tilde{T}(\varphi,\theta)\cos^2(\alpha-\theta), \quad (4)$$

where $\tilde{T}(\varphi,\theta)$ is the tunneling probability $T(S)$ for a molecule rotated by φ and θ with reference to the TDM and N the corresponding normalization factor.

The measured and calculated values for the angle-dependent ionization are shown in Fig. 1. The data are recorded for zero time delay. Similar observations have been obtained for different time delays and are discussed in detail in Ref. [23]. The angular dependence seen in the ionization yield for AT varies slightly with intensity, with the anisotropy decreasing with decreasing probe intensity, but persisting for even the lowest intensities where signal is observed [23]. While the measurements were carried out in a regime of mixed multiphoton and tunnel character, the calculations focus on tunnel ionization after $\pi\pi^*$ excitation, neglecting the multiphoton character in the experimental ionization. This explains the slight deviations from experiment but illustrates that tunnel ionization is key to the observed anisotropic behavior. Although the π and π^* orbitals of all three molecules have a very similar shape, differences in the angle-dependent tunnel ionization (ADTI) are observed, in theory as well as in experiment. The tunnel ionization for CHD is almost perfectly isotropic. The same is observed for AP, while, surprisingly, AT shows a distinct anisotropy.

To understand this behavior, we analyze the field-dressed molecular orbitals and discuss the reason for the observed anisotropy in detail for the case of AT. The strong probe pulse (Fig. 2, red) ionizes the excited-state molecules and the angle dependence is recorded. Figure 2 shows the ionization pulse and molecule for two values of α, 0° and 90°, for which there is the largest contrast in the ADTI of AT. For clarity, we show the molecules whose TDM are oriented exactly along the pump pulse polarization. We observe the following differences: For CHD and AP the sp^2 C-H bonds (indicated by dark red circles) line up along the polarization axis of the ionization pulse for both α values, while in AT this is only the case for $\alpha = 90°$. For $\alpha = 0°$ an sp^3 C-H bond (olive circle) exists along the probe direction.

sp^2 bonds are more easily polarized than sp^3 bonds due to their π-orbital character. Polarizability is an important factor in tunnel ionization with strong fields. If the excited state prepared with the pump pulse becomes polarized in the strong field of the probe pulse, then there will be more ionization. If the polarization depends on the angle α, then the strong-field ionization yield will also depend on the angle. Depending on the molecule, strong-field interaction can significantly mix and distort the orbitals in a way that depends on the angle of the field relative to the molecule [20]. In the case of the small organic molecules, it is important to consider the presence of low-lying Rydberg orbitals (see Fig. 3 for AT), already in

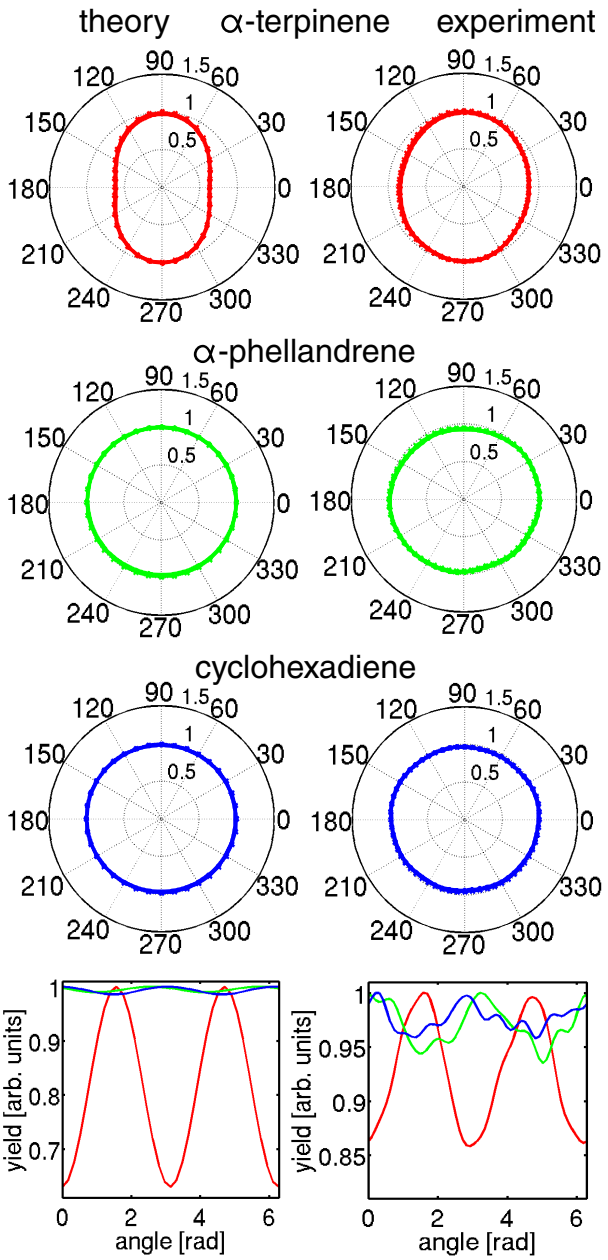

FIG. 1. (Color online) Calculated (left) and measured (right) angle-dependent ionization yields for α-terpinene (red), α-phellandrane (green), and cyclohexadiene (blue). Measurements are presented for zero time delay between pump and probe pulses. Similar results were obtained for small positive delays between pump and probe pulses. The bottom two panels show the calculated (left) and measured (right) ionization yields as a function of angle between pump and probe pulses for all three molecules. Experimental uncertainties are about 2% of the yields.

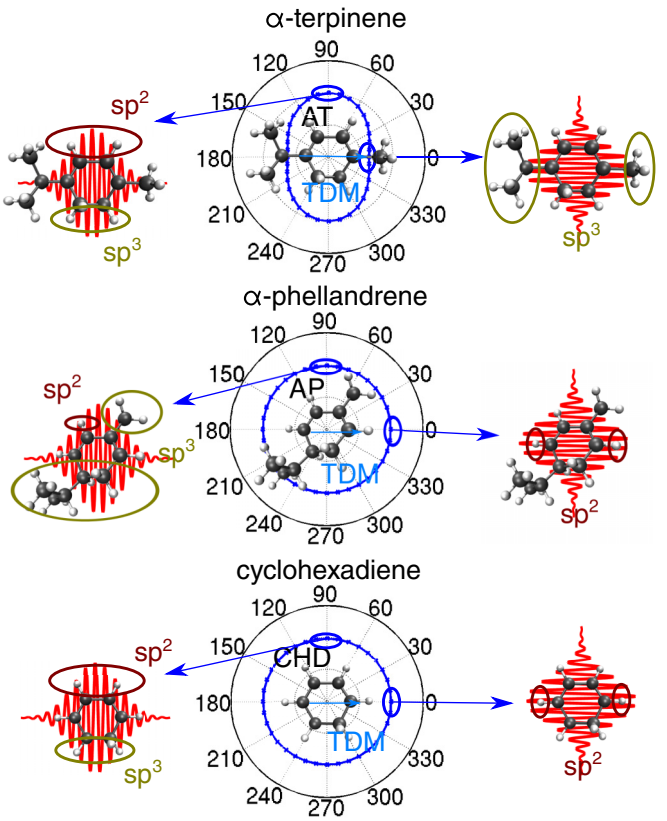

FIG. 2. (Color online) Calculated angular-dependent ionization yields $\tilde{T}(\alpha)$ for AT, AP, and CHD shown in the middle column. CHD shows the most isotropic angular dependence, AP is almost isotropic, and AT is anisotropic. On the left- and right-hand sides, the molecules are shown along with the ionization pulse for two selected angles between the pump and probe pulses ($\alpha = 0°$ and 90°). The molecular transition dipole moment is oriented exactly along the pump-pulse polarization vector. The selected angles correspond to the axis of anisotropy for AT. For both α values AP and CHD have sp^2 C-H bonds (indicated by dark red circles) along the direction of the probe pulse. In contrast, AT has only sp^3 C-H bonds (indicated by olive circles) along the direction of the probe laser for $\alpha = 0°$, while for $\alpha = 90°$ again sp^2 C-H bonds are present.

the field-free molecules. This is different for most diatomics. Rydberg orbitals are diffuse and easy to polarize, thus they will enhance tunnel ionization. The degree of orbital mixing and its angle dependence is determined in large part by whether sp^3 or sp^2 orbitals line up along the laser polarization. sp^3 bonds will mix less with Rydberg orbitals compared with sp^2 bonds. AT has sp^2 orbitals only perpendicular to the TDM and thus a larger difference in the perpendicular vs parallel ADTI signal than the other two molecules. This interpretation is based upon an analysis of field-dressed orbitals. Orbital mixing induced by the ionization pulse is shown for the most interesting case of AT in Fig. 3.

For all α values the strong field stabilizes the originally delocalized LUMO (Rydberg, blue line) orbital into a localized version pointing into the direction of the light field. In the case where the laser direction coincides with the direction of an sp^2 (or sp) C-H bond, an additional, originally-higher-lying Rydberg orbital (red line) is stabilized close to the energy of the π orbital (black line). This stabilization leads to an equivalent occupation of the π orbital and LUMO+1 orbitals in the excited-state configuration. This scenario is shown for $\alpha = 90°$. Our calculations show that the mixing in of the Rydberg character leads to a large tunneling rate for the LUMO+1 in

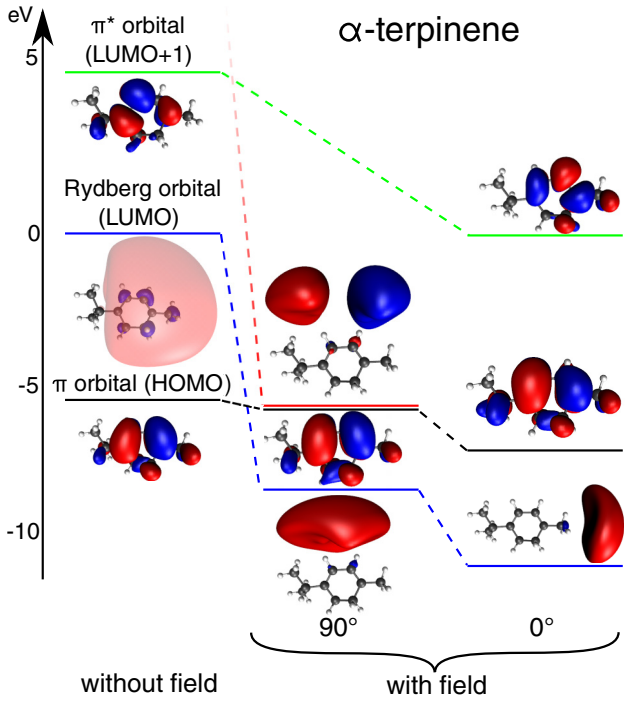

FIG. 3. (Color online) State-averaged CASSCF molecular orbitals from which an electron is removed for α-terpinene, giving rise to anisotropy in the angular ionization rate. Without field the π orbital is the HOMO (black line), the Rydberg orbital is the LUMO (blue line) and the $\pi*$ orbital is the LUMO+1 (green line). We use dashed lines to indicate the correlations of the orbitals with and without field. For all α values the light field stabilizes the originally delocalized LUMO (Rydberg) orbital into a localized version pointing in the direction of the light field. When the laser direction coincides with the direction of an sp^2 (or sp) C-H bond, an additional, originally-higher-lying Rydberg orbital (red line) is stabilized close in energy to the π orbital. This scenario is shown for $\alpha = 90°$. For $\alpha = 0°$ the laser direction coincides with the direction of the sp^3 C-H bond and the additional higher-lying Rydberg orbital is not stabilized.

that direction. The laser-stabilized π orbital contributes very little to the angle-dependent ionization rate. For $\alpha = 0°$ the situation is changed. Now the laser direction coincides with the direction of the sp^3 C-H bond and the additional higher-lying Rydberg orbital is not stabilized, therefore not occupied and thus leading to less ionization probability in this direction. For CHD and AP the $\alpha = 0°$ case is similar to the $\alpha = 90°$ case and the LUMO+1 always has Rydberg character. As the tunneling also depends on the energy of the orbital, the low-lying field-dressed HOMO–1 orbital with strong Rydberg character does not participate.

We have considered the role of Stark-shifted or field-dressed molecular orbitals in describing strong-field ionization of polyatomic molecules from the first excited state. Our calculations of the angle-dependent ionization yield agree well with measurements and indicate that in contrast to smaller less polarizable molecules, field-dressed orbitals need to be taken into account in order to capture the measured angle-dependent yields.

For some molecules, particularly small ones that are not very polarizable (such as N_2), the field-free orbitals and states are not affected as much by the strong field. This is different from the case of the small organic molecules we considered. Here the field can significantly mix and distort the orbitals in a way that depends on the angle of the field relative to the molecule. The reason lies in the low-lying Rydberg orbitals that exist already in the field-free molecules for all three systems. The observed differences are determined in large part by whether sp^3 or sp^2 orbitals line up along the polarization axis of the ionization field.

R.d.V.-R. and R.S. gratefully acknowledge financial support from the Deutsche Forschungsgemeinschaft through the SFB749 and the cluster of excellence Munich-Centre for Advanced Photonics (MAP). T.W. gratefully acknowledges support from the Department of Energy under Grant No. DEFG02-08ER15983.

[1] M. Y. Ivanov, M. Spanner, and O. Smirnova, J. Mod. Opt. **52**, 165 (2005).
[2] Y. Mairesse *et al.*, Phys. Rev. Lett. **104**, 213601 (2010).
[3] T. Popmintchev, M.-C. Chen, P. Arpin, M. M. Murnane, and H. C. Kapteyn, Nat. Photon. **4**, 822 (2010).
[4] M. F. Kling and M. J. Vrakking, Annu. Rev. Phys. Chem. **59**, 463 (2008).
[5] Z. Chang and P. Corkum, J. Opt. Soc. Am. B **27**, B9 (2010).
[6] P. Agostini and L. F. DiMauro, Rep. Prog. Phys. **67**, 813 (2004).
[7] R. Kienberger, M. Uiberacker, M. F. Kling, and F. Krausz, J. Mod. Opt. **54**, 1985 (2007).
[8] W. Li, A. A. Jaroń-Becker, C. W. Hogle V. Sharma, X. Zhou, A. Becker, H. C. Kapteyn, and M. M. Murnanea, Proc. Natl. Acad. Sci. U.S.A. **107**, 20219 (2010).
[9] L. Holmegaard *et al.*, Nat. Phys. **6**, 428 (2010).
[10] T. K. Kjeldsen, C. Z. Bisgaard, L. B. Madsen, and H. Stapelfeldt, Phys. Rev. A **68**, 063407 (2003).
[11] J. Itatani, J. Levesque, D. Zeidler, H. Niikura, H. Pépin, J. C. Kieffer, P. B. Corkum, and D. M. Villeneuve, Nature (London) **432**, 867 (2004).
[12] I. V. Litvinyuk, K. F. Lee, P. W. Dooley, D. M. Rayner, D. M. Villeneuve, and P. B. Corkum, Phys. Rev. Lett. **90**, 233003 (2003).
[13] A. S. Alnaser, C. M. Maharjan, X. M. Tong, B. Ulrich, P. Ranitovic, B. Shan, Z. Chang, C. D. Lin, C. L. Cocke, and I. V. Litvinyuk, Phys. Rev. A **71**, 031403 (2005).
[14] A. Fleischer, H. J. Wörner, L. Arissian, L. R. Liu, M. Meckel, A. Rippert, R. Dörner, D. M. Villeneuve, P. B. Corkum, and A. Staudte, Phys. Rev. Lett. **107**, 113003 (2011).
[15] D. Pavicic, K. F. Lee, D. M. Rayner, P. B. Corkum, and D. M. Villeneuve, Phys. Rev. Lett. **98**, 243001 (2007).
[16] A. S. Alnaser, S. Voss, X. M. Tong, C. M. Maharjan, P. Ranitovic, B. Ulrich, T. Osipov, B. Shan, Z. Chang, and C. L. Cocke, Phys. Rev. Lett. **93**, 113003 (2004).

[17] O. Smirnova, S. Patchkovskii, Y. Mairesse, N. Dudovich, and M. Y. Ivanov, Proc. Natl. Acad. Sci. U.S.A. **106**, 16556 (2009).
[18] I. Znakovskaya, P. von den Hoff, S. Zherebtsov, A. Wirth, O. Herrwerth, M. J. J. Vrakking, R. de Vivie-Riedle, and M. F. Kling, Phys. Rev. Lett. **103**, 103002 (2009).
[19] H. Akagi, T. Otobe, A. Staudte, A. Shiner, F. Turner, R. Dörner, D. M. Villeneuve, and P. B. Corkum, Science **325**, 1364 (2009).
[20] P. von den Hoff, I. Znakovskaya, S. Zherebtsov, M. F. Kling, and R. de Vivie-Riedle, Appl. Phys. B **98**, 659 (2009).
[21] Z. X. Zhao, X.-M. Tong, and C.-D. Lin, Phys. Rev. A **67**, 043404 (2003).
[22] M. Kotur, T. C. Weinacht, C. Zhou, and S. Matsika, Phys. Rev. X **1**, 021010 (2011).
[23] O. Njoya, S. Matsika, and T. Weinacht, ChemPhysChem **14**, 1451 (2013).
[24] D. Dimitrovski, C. P. J. Martiny, and L. B. Madsen, Phys. Rev. A **82**, 053404 (2010).
[25] E. Wells *et al.*, Nat. Commun. **4**, 2895 (2013).
[26] H.-J. Werner, P. J. Knowles, G. Knizia, F. R. Manby, M. Schütz, P. Celani, T. Korona, R. Lindh, A. Mitrushenkov, and G. Rauhut, MOLPRO, version 2012.1, a package of *ab initio* programs, 2012.
[27] B. M. Smirnov and M. I. Chibisov, Sov. Phys. JETP **22**, 585 (1966).
[28] I. Barth, H.-C. Hege, H. Ikeda, A. Kenfack, M. Koppitz, J. Manz, F. Marquardt, and G. K. Paramonov, Chem. Phys. Lett. **481**, 118 (2009).
[29] P. E. Share, K. L. Kompa, S. D. Peyerimhoff, and M. C. van Hemert, Chem. Phys. **120**, 411 (1988).
[30] D. Geppert and R. de Vivie-Riedle, Chem. Phys. Lett. **404**, 289 (2005).